Electronic Supplementary Material (ESI) for Lab on a Chip.

SUPPLEMENTAL FIGURES

SUPPLEMENTAL TABLE 1. FWHM measurements of PSFs

			FWHM Measurements (μm)			
Imaging Mode	Position of Bead	Stock FEP Thickness	X	Y	Z	Strehl Ratio
Angled Widefield	On top of FEP	NA	0.38 ± 0.01	0.38± 0.00	1.38 ± 0.03	NA
	In Chip	12.5 μm	0.37 ± 0.00	0.46 ± 0.01	1.38 ± 0.08	0.7097
		25 μm	0.37 ± 0.01	0.48 ± 0.01	1.37 ± 0.03	0.4384
		50 μm	0.39 ± 0.01	0.54 ± 0.01	1.43 ± 0.01	0.4212
Lattice Light Sheet	On top of FEP	NA	0.39 ± 0.00	0.37 ± 0.01	0.82 ± 0.03	NA
	In Chip	12.5 μm	0.37 ± 0.00	0.47 ± 0.01	0.83 ± 0.01	0.7857
		25 μm	0.37 ± 0.00	0.49 ± 0.01	0.83 ± 0.02	0.5108
		50 μm	0.41 ± 0.03	0.54 ± 0.01	0.88 ± 0.01	0.5783

*n=3 beads for each condition

SUPPLEMENTAL TABLE 2. Description of imaging parameters

Figure	**Lattice Type**	**Outer NA**	**Inner NA**	**Wavelength (nm)**	**Power* (μW)**	**Exposure Time (ms)**	**Volumetric Sampling Interval (min)**	**X-stage step size (nm)**
4A	Square	0.30	0.25	642	20	40	5	750
4B	Square	0.35	0.30	642	256	50	5	500
4C	Square	0.30	0.25	642	128	30	1.5	400
4D	Square	0.35	0.30	642	31	30	7	500
5A	Square	0.40	0.30	560	93	25	2	500
5B	Square	0.40	0.30	560	57	30	5	500
6A-B	Hexagonal	0.55	0.50	560	70	50	6	400
6C-E†	Square	0.40	0.30	642	38000	30	0.08	500

*Power measured at the rear pupil of the excitation objective.

SUPPLEMENTAL FIGURE 1

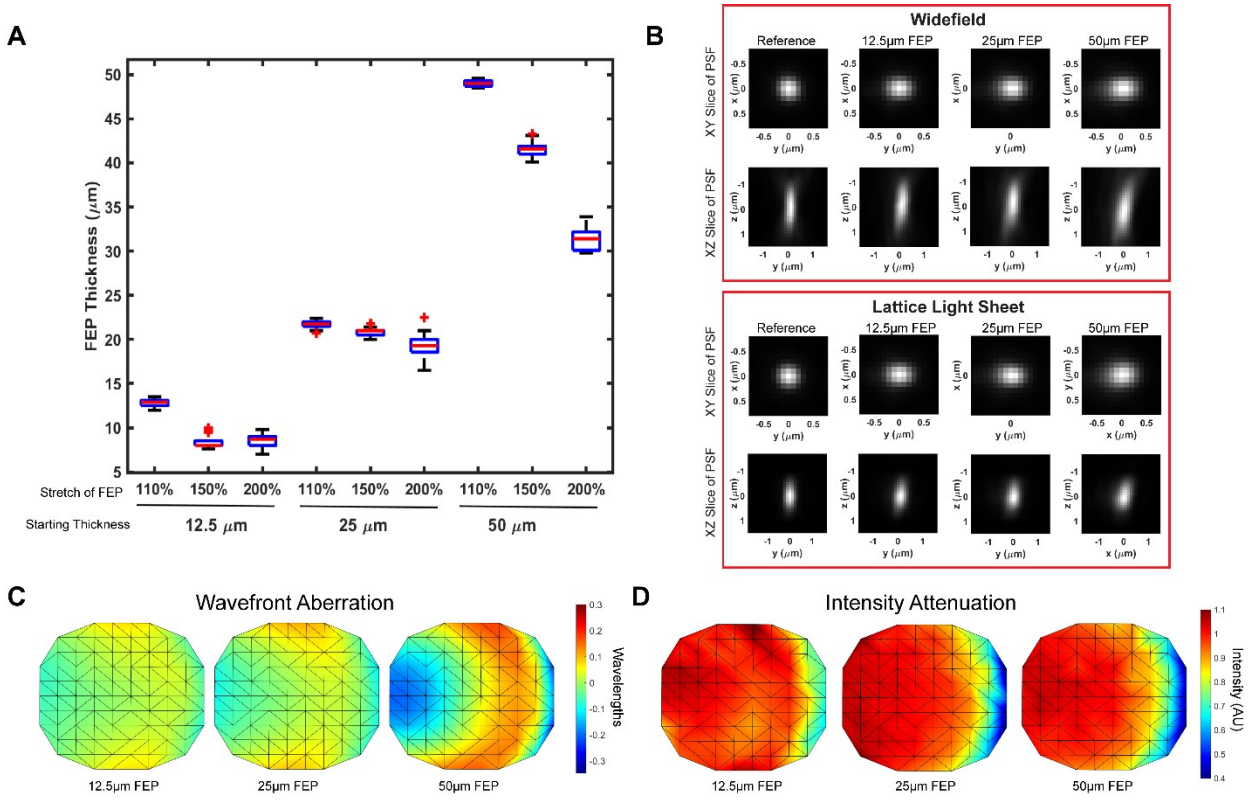

Supplemental Figure 1. Further characterization of microfluidic chip. A) The FEP thickness can be reduced via stretching. For 12.5 µm at 110% stretch n=18 measurements in one chip; for 12.5 µm at 150% stretch n=16 measurements in one chip and n=5 measurements in a second chip; for 12.5 µm at 200% stretch n=15 measurements in one chip and 5 measurements in a second chip. For 25 µm at 110% stretch n=18 measurements in one chip; for 25 µm at 150% stretch n=16 measurements in one chip and n=5 measurements in a second chip, for 25 µm at 200% stretch n=16 measurements in one chip and 5 measurements in a second chip. For 50 µm at 110% stretch n=18 measurements in one chip; for 50 µm at 150% stretch n=16 measurements in one chip and n=5 in a second chip; for 50 µm at 200% stretch n=5 measurements in one chip. **B)** PSF images for films of different thickness under 110% stretch. The PSF widens along the Y axis as the film thickness increases. **C)** Increasing the FEP film thickness increases the aberration of the wavefront. **D)** In contrast, there is minimal increase in intensity attenuation as the film thickness increases. *Note that due to refraction at the film interface, there would be an apparent defocus and lateral shift in the optimal focus when imaging through the film. Based on CodeV simulations, we estimate that this shift would cause our experimental thickness measurements to be overestimated by approximately 2.6% of the true film thickness.

SUPPLEMENTAL FIGURE 2

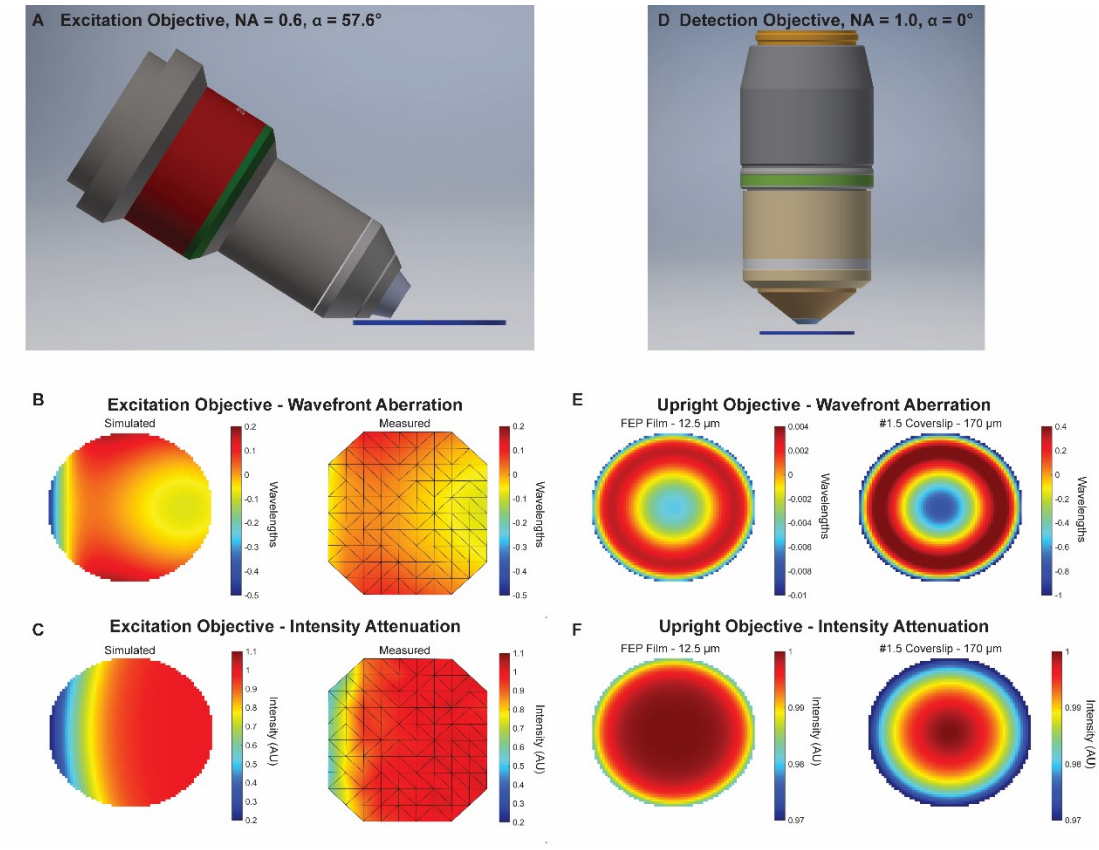

Supplemental Figure 2. Film-induced Optical Aberrations in other optical scenarios. A) Schematic demonstrating the orientation of the excitation objective relative to the sample for optical simulations. **B)** Wavefront abberation generated by the FEP film when illuminated with the excitation objective (NA = 0.6, α_{exc} = 57.6°). Modeled aberration in wavelengths that the FEP introduces to the wavefront using the optics software Code V (left). Measured abberation of the wavefront generated by the FEP film using a Shack-Hartman sensor (right). **C)** Intensity attenuation due to the presence of the FEP film when illuminated with the excitation objective (NA = 0.6, α_{exc} = 57.6°). Relative intensity of light after passing through the film, modeled in Code V (left). Measured intensity using a Shack-Hartmann sensor (right). **D)** Schematic demonstrating an upright detection objective relative to the sample for optical simulations. **E)** Simulated wavefront aberration when illuminated with an upright detection objective (NA = 1.0, α = 0°) with rays traveling through the FEP film (RI = 1.345, thickness = 12.5 µm, left) or through a #1.5 coverslip (RI = 1.52, thickness = 170 µm, right). **F)** Simulated intensity attenuation when illuminated with an upright detection objective (NA = 1.0, α = 0°) with rays traveling through the FEP film (RI = 1.345, thickness = 12.5 µm, left) or through a #1.5 coverslip (RI = 1.52, thickness = 170 µm, right).

SUPPLEMENTAL FIGURE 3

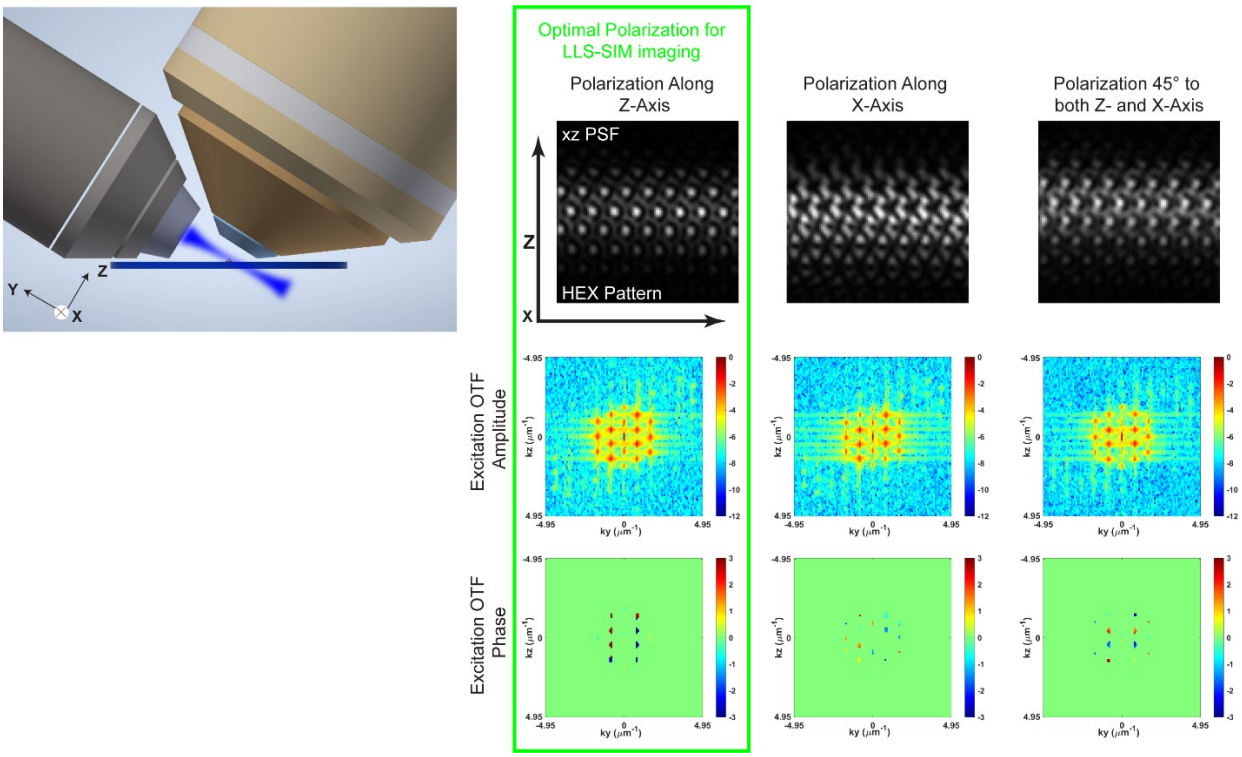

Supplemental Figure 3. Interaction between chip orientation and polarization of excitation beam. When imaging, the fast axis (direction of uniaxial stretch of FEP) of the chip is oriented along the x-axis. High-contrast modulation of the excitation pattern for SIM imaging is optimal when the excitation light is polarized along the z-axis. Non-optimal polarization causes the excitation orders to obtain a complex axial phase dependence that would interfere with conventional SIM reconstruction algorithms.

SUPPLEMENTAL FIGURE 4

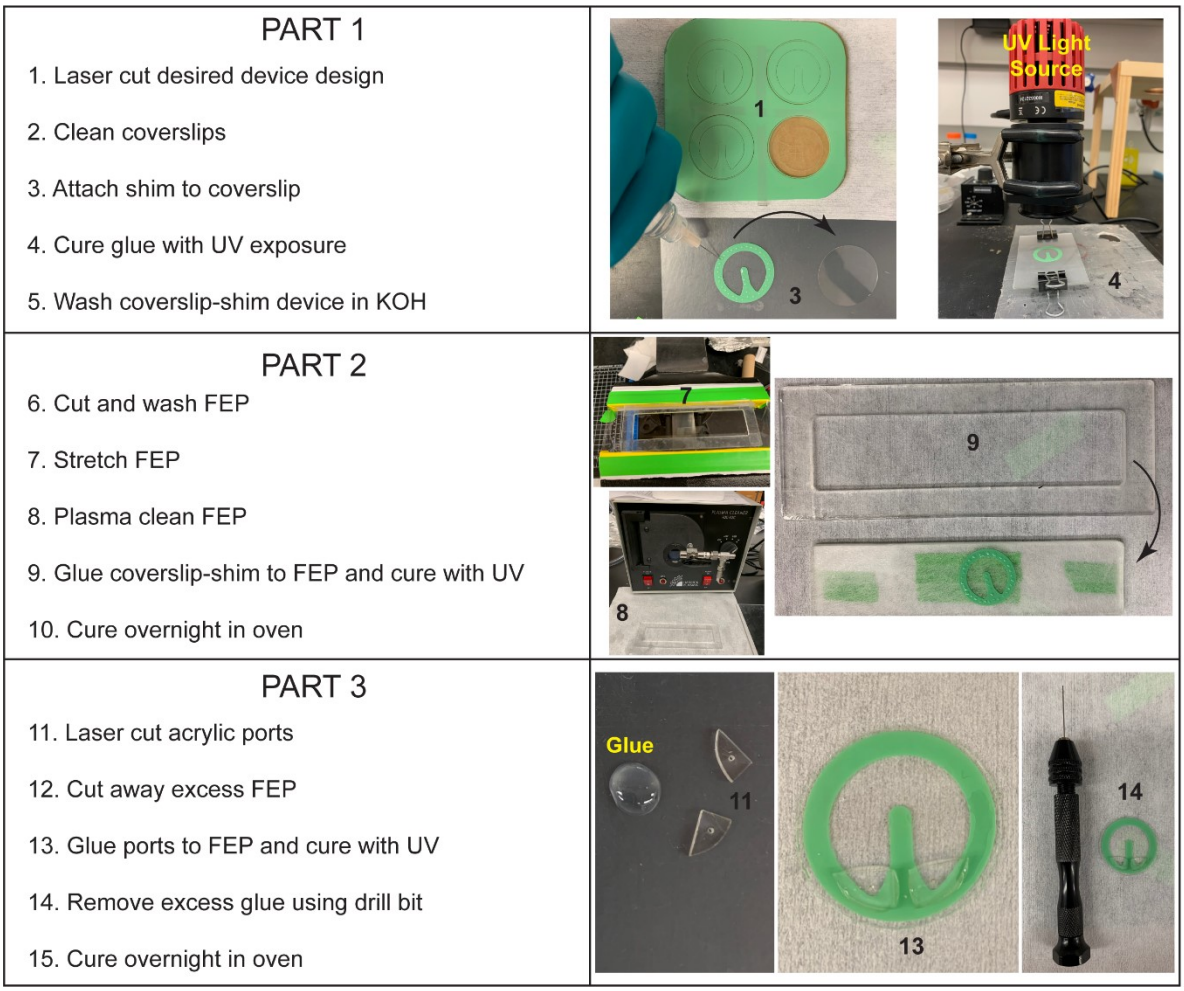

Supplemental Figure 4. Assembly of microfluidic chip. An outline of the key steps in the fabrication and assembly of our microfluidic chip. In Part 1, the main body of the chip is assembled from a #1.5, 25 mm coverslip and 76.2 µm thick polyester shim stock. The coverslip/shim assembly can be stored and saved for later manufacturing. In Part 2, the top FEP film layer is washed, stretched, plasma treated, and glued to the shim of the previously assembled device. In Part 3, the acrylic ports are added to allow loading and fluid exchange in the chip.

SUPPLEMENTAL MOVIE LEGENDS

Supplemental Movie 1. Megakaryocytes in late pro-platelet formation have dynamic cellular protrusions. Volume rendering of MKs in late pro-platelet formation demonstrates highly dynamic, thin cellular protrusions prior to budding into pro-platelets. MKs labeled with anti-GPIX-647 and imaged with lattice light sheet microscopy. The cubic scale bar covers a 10 μm x 10 μm x 10 μm volume.

Supplemental Movie 2. Protrusion growth during mid pro-platelet formation. Volume rendering of MKs in mid pro-platelet formation demonstrates growth of cellular protrusions. MKs labeled with anti-GPIX-647 and imaged with lattice light sheet microscopy. The cubic scale bar covers a 2 μm x 2 μm x 2 μm volume.

Supplemental Movie 3. Microfluidic device allows rapid application and washout of Blebbistatin. U2OS cells expressing Lifeact::RFP were seeded in the microfluidic chip and imaged on a lattice light sheet microscope prior to the application of 50 μM Blebbistatin. This resulted in the rapid disassembly of stress fibers and change in cellular morphology. Upon washout, the stress fibers recovered and cells returned to their normal morphology.

Supplemental Movie 4. Cells were viable and imaged long-term in the microfluidic chips. U2OS cells expressing Lifeact::RFP were imaged in the microfluidic chip for 12 hours during which time they retained normal cell morphology and behavior.

Supplemental Movie 5. Microfluidic chips are compatible with live-cell super resolution SIM imaging. We imaged Lifeact::RFP expressing U2OS cells using LLS-SIM for 2 hours. Images were reconstructed using both SIM-reconstruction and deconvolution as described in the methods.

Supplemental Movie 6. Volume rendering of DNA PAINT dataset in microfluidic chip. Super-resolution imaging of DNA PAINT within the microfluidic chip. Probes were used in conjunction with antibodies against Lamin A/C and H3K27ac. The bounding box in the movie has dimensions of 14.4 μm x 15.3 μm x 5.22 μm.